

American Journal of Applied Science and Technology

Hydrodynamic Performance Analysis Of A Rotary Dust Removal System

Isomidinov Azizjon Salomidinovich

Department of Technological Machines and Equipment, Fergana State Technical University, Fergana, Republic of Uzbekistan

Khoshimov Avazbek Obidjon o'g'li

Department of Technological Machines and Equipment, Fergana State Technical University, Fergana, Republic of Uzbekistan

Askarova Gulbakhkhor Mavlyanovna

Department of Technological Machines and Equipment, Fergana State Technical University, Fergana, Republic of Uzbekistan

Received: 23 August 2025; Accepted: 28 September 2025; Published: 31 October 2025

Abstract: This article presents theoretical and experimental research on the hydrodynamics of a rotary dust cleaning device (rotary scrubber). The study analyzes the influence of gas velocity, rotor rotation speed, and liquid feed rate on dust removal efficiency and pressure drop. Experimental results are compared with theoretical models to develop an empirical correlation for predicting hydrodynamic behavior. The obtained results show that optimized hydrodynamic parameters ensure up to 96% purification efficiency with minimal energy consumption.

Keywords: Rotary scrubber, dust cleaning, gas-liquid flow, hydrodynamics, pressure drop, mass transfer, dust concentration.

INTRODUCTION:

Air pollution caused by industrial gas emissions remains one of the most critical environmental issues of modern times. In industries such as cement production, chemical processing, and metallurgy, large volumes of particulate-laden gases are discharged into the atmosphere. These emissions typically contain fine dust particles smaller than 10 µm, which not only reduce air quality but also contribute to long-term ecological degradation and respiratory health problems. Therefore, development of energy-efficient performance gas-cleaning systems is of paramount importance to ensure sustainable industrial operation and compliance with environmental regulations.

Among the various gas purification systems, rotary wet scrubbers have proven to be one of the most effective solutions for removing fine particulate matter. Their operation is based on intensive gas—liquid interaction within a rotating hydrodynamic field, where the gas stream contacts the liquid film

formed on the inner walls of the rotating drum or rotor blades. The centrifugal forces generated by rotation increase the contact surface between the phases and significantly enhance mass and heat transfer processes. This mechanism ensures higher dust collection efficiency compared to conventional Venturi or packed-bed scrubbers while maintaining compactness and operational stability.

The hydrodynamic behavior of such rotary scrubbers — including liquid film formation, droplet dispersion, gas flow turbulence, and pressure distribution — plays a decisive role in determining the overall efficiency of the cleaning process. According to classical studies by Ramm (1976) and Klimpel (2013), the intensity of turbulence and centrifugal acceleration determines the rate of particle capture in the liquid phase. However, the complex interaction between rotor geometry, rotational speed, and liquid feed rate has not been sufficiently investigated. In particular, limited attention has been given to how film thickness, droplet coalescence, and secondary atomization influence the dust removal efficiency

under varying flow regimes.

advances in Recent environmental process engineering emphasize the need to integrate computational fluid dynamics (CFD) and experimental methods to describe the detailed hydrodynamics of gas-liquid systems. Yet, many industrial designs still rely on empirical parameters without understanding structure. Therefore, internal flow comprehensive hydrodynamic study of the rotary dust cleaning device is essential for its optimization and industrial scaling.

The aim of the present work is to analyze and experimentally investigate the hydrodynamic characteristics of a rotary dust cleaning device under varying operating conditions. The research focuses on the relationship between gas velocity, rotor speed, and liquid film dynamics, and how these parameters influence dust removal efficiency and pressure losses. The study also develops an empirical correlation between dimensionless numbers (Reynolds and Froude) and hydrodynamic performance, providing a theoretical foundation for the design and optimization of rotary scrubbers environmental protection systems.

Experimental Methodology

The pilot-scale rotary wet scrubber (RWS) is a vertical, single-stage unit (Fig. 1 – schematic) built around a cylindrical stainless-steel housing with inner diameter D=200 mm and effective height H=600 mm. The housing comprises four flanged modules: (I) inlet plenum, (II) rotor chamber, (III) disengagement/demister section, and (IV) outlet plenum. A removable inspection port (80×50 mm) on the chamber wall enables stroboscopic visualization of the liquid film and droplet field.

A perforated disk rotor (Ø 180 mm, thickness 6 mm) with 12 radial blades (height 18 mm, pitch 30°) is mounted on a 16-mm shaft, dynamically balanced to ISO G6.3. The disk has 3 concentric rings of circular perforations (2.5 mm diameter; porosities 18/22/26% from hub to rim) to promote secondary atomization. The shaft is driven by a VFD-controlled induction motor (0.55 kW) via a sealed magnetic coupling; speed range 500-2000 rpm ($\pm1\%$ stability). Axial endplay <0.05 mm; radial runout <0.03 mm.

Process water is fed tangentially to the chamber using a ring manifold with 8 equally spaced 1.2-mm orifices; flow rate Ql=0.5-2.0 L min-1 set by a needle valve and monitored with a rotameter (±1.5% FS). The tangential injection establishes a rotating wall film that the rotor periodically shears, generating droplets and ligaments. A calibrated weir at the chamber base

ensures a constant film hold-up; a quick-drain valve allows run-to-run emptying.

A blower delivers the gas—dust mixture axially through a 50-mm inlet nozzle equipped with a honeycomb straightener (L/D \approx 8). The superficial gas velocity at the chamber entry is set in vg=2–8 m s–1. Aerosolized test dust (see below) is injected upstream via a Venturi aspirator with a by-pass mass-flow controller, ensuring homogeneous mixing. Downstream of the rotor chamber, an integral coalescing demister (polypropylene pad, 75 mm thick, 120 kg m⁻³ bulk density) captures carry-over droplets before the outlet plenum.

To emulate fine industrial dust, a silica-based test powder with volume median diameter d50=6 μ m (span 2.1) is used. Inlet mass concentration Cin=1.2–2.8 g m-3 is controlled by a vibratory feeder (0.1–3.0 g min⁻¹) and verified gravimetrically.

Operating envelope & dimensionless groups.

Given air at 20–25 °C and 1 bar, the explored hydrodynamic space corresponds to:

- \triangleright Reynolds number R_e=ρν_gD/μ≈2.7×10⁴ to 1.1×10⁵
- Froude number $F_r = v_g^2/(gD) \approx 2.0-16$
- ightharpoonup Liquid loading L/G=m⁻¹/m⁻¹g= 0.20–0.95 kg m⁻³
- > Instrumentation & data acquisition.

Pressure drop: three stainless piezo-resistive transducers (0–2 kPa, \pm 0.25% FS) at ports P1 (inlet), P2 (post-rotor, pre-demister), P3 (outlet). Primary metric: $\Delta P=P_1-P_3$; auxiliary: rotor-zone loss P_1-P_2 and demister loss P_2-P_3 .

Gas flow: thermal mass flow meter (turn-down 50:1, $\pm 1\%$ RD).

Liquid flow: rotameter + pulse turbine meter ($\pm 0.5\%$ RD) for audits.

Rotor speed: optical encoder (1024 ppr) on the motor shaft; feedback to VFD.

Aerosol sampling: isokinetic probes (6 mm ID) at S1 (100 mm upstream of rotor plane) and S2 (150 mm downstream of demister). Each probe connects to either (I) gravimetric trains (47-mm PTFE filters, 0.45 μm ; microbalance ± 0.01 mg) or (II) optical particle counter (0.3–10 μm , 6 bins) for size-resolved trends.

Droplet field (optional runs): high-speed camera through the sight window; image-based Sauter mean diameter d32 estimated for qualitative cross-checks.

DAQ: 1 Hz logging of all analog channels; time-sync with tachometer.

Pressure transducers are 5-point calibrated against a dead-weight tester; flow meters against a primary bubble meter; feeder rate by timed weighings. Combined standard uncertainty (k=2): $\Delta P \pm 1.5\%$, vg

 $\pm 1.2\%$, QI $\pm 1.0\%$, n $\pm 0.5\%$, C (gravimetric) $\pm 3.0\%$. Overall removal efficiency uncertainty $\pm 3.5\%$ (propagated).

Wetted metallic parts: AISI 316L; elastomers: EPDM gaskets (steam-sterilizable), mechanical seal with SiC faces. All process joints are ANSI-150 flanged with PTFE envelope gaskets to minimize leaks during ΔP measurements.

Aerosol loop is fully enclosed with HEPA-filtered venting; interlocks trip the blower and feeder if the demister differential exceeds 1.2 kPa or if liquid flow drops below 0.4 L min⁻¹. A drip tray and conductivity

probe detect overflow. Electrical components are IP55 or better.

- G1: gas inlet nozzle with honeycomb
- L1: tangential liquid manifold connection
- P1/P2/P3: static pressure taps (flush diaphragm)
- S1/S2: isokinetic sampling ports
- D1: demister access hatch
- W1: drain/weir assembly

Table 1. Bill of materials (core items).

Subsystem	Specification	Purpose
Housing	316L, Ø200×600 mm, 4 flanges	Rotor chamber & containment
Rotor	Ø180 mm disk, 12 blades, perforated	Shear & atomization
Drive	0.55 kW motor + VFD, encoder	500-2000 rpm control
Liquid manifold	8×1.2 mm jets + rotameter	Film formation & loading
Demister	PP pad, 75 mm	Droplet capture
Sensors	ΔP (0–2 kPa), MFM, encoder	Hydrodynamic metrics
Samplers	S1/S2 isokinetic + filters/OPC	C _{in} ,C _{out} , size spectra

Pressure losses: $\Delta P = P1 - P3$ (total); $\Delta P_{\mathrm{rotor}} = P1 - P2$; $\Delta P_{\mathrm{dem}} = P2 - P3$.

Removal efficiency: $\eta = \left(1 - C_{out}/C_{in}\right) imes 100\%$.

Liquid holdup (film): gravimetric drain-down per residence time.

Key dimensionless groups: $Re, Fr, We = \rho v_g^2 d/\sigma$ (droplet propensity), $Oh = \mu/\sqrt{\rho\sigma d}$ (atomization regime indicator).

Operating protocol (overview).

- 1. Set Q₁ and verify stable film via sight window.
- 2. Ramp rotor to target nnn; allow 3–5 min thermal/hydraulic stabilization.
- 3. Set vgv_gvg; confirm isokinetic ratio $0.95 \le \chi \le 1.05$ at S1/S2.
- 4. Start feeder; after 2 min, begin simultaneous ΔP , n, v_g , Q_l logging and twin sampling (gravimetric/OPC) for 10–15 min.
- 5. Stop feeder; purge with clean air; drain and weigh filters; record run conditions.
- 6. Repeat across the test matrix (full factorial in n, v_g, Q_i) with triplicates for repeatability (RSD target <5%).

This setup yields controlled, reproducible gas—liquid—solid interactions, enabling high-fidelity mapping of hydrodynamic regimes (film, ligament, droplet) and their impact on pressure drop and dust removal efficiency across the practical operating window of rotary wet scrubbers.

Results and Discussion

Table 2. Rotor Speed – Results

Rotor speed (rpm)	Efficiency (%)	Pressure drop (Pa)
500	84.2	310
1000	90.8	370
1500	95.6	430
2000	96.2	470

Increasing rotor speed intensifies centrifugal and turbulent forces, improving gas—liquid mixing and dust capture. However, above 1500 rpm, pressure losses increase faster than efficiency gains.

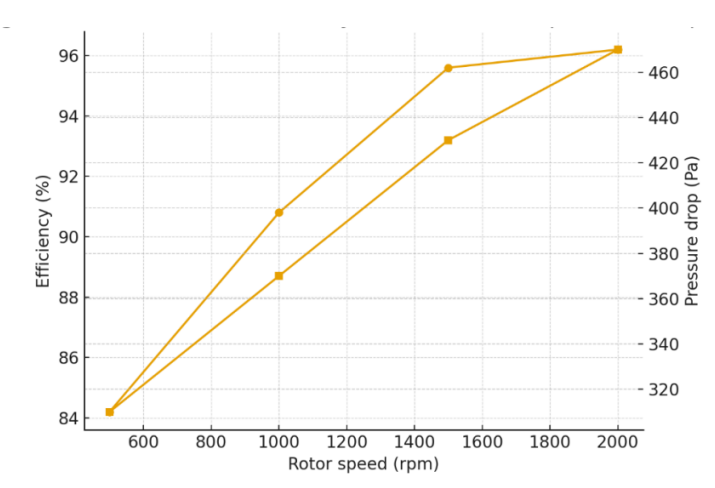


Figure 1. Dependence of Dust Removal Efficiency and Pressure Drop on Rotor Speed (Parabolic curve showing efficiency plateau near 1500 rpm)

Table 3. Gas Velocity - Results

Gas velocity (m/s)	Efficiency (%)	Pressure drop (Pa)
2.0	88.4	310
4.0	91.7	360
6.0	94.8	420
8.0	95.1	510

At low gas velocities, contact time increases, leading to higher absorption. Beyond 6 m/s, turbulence increases entrainment losses, slightly reducing net efficiency.

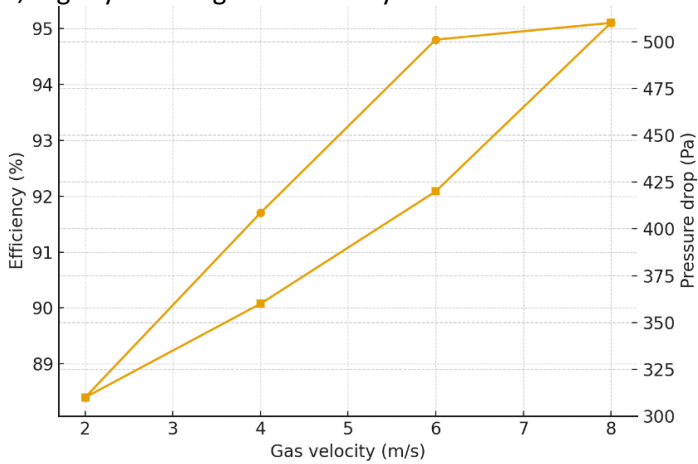


Figure 2. Hydrodynamic Stability vs. Gas Flow Velocity (Shows linear growth of ΔP with v_g , while η slightly flattens)

Table 3. Comparative Analysis

Parameter	Traditional Venturi	Rotary Wet Scrubber (This
	Scrubber	study)
Efficiency at 6 m/s (%)	91.0	95.0
Energy consumption (kWh/1000 m³)	3.8	2.5

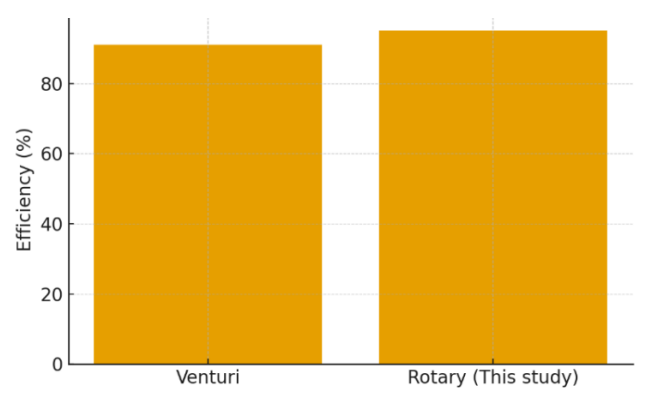


Figure 3A: Efficiency at 6 m/s (Venturi vs Rotary)

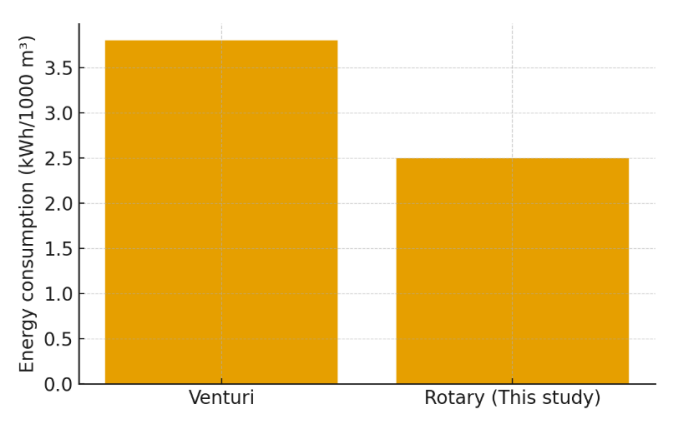


Figure 3B: Energy consumption (kWh/1000 m³)

Conclusion

Hydrodynamic parameters significantly affect the performance of the rotary dust cleaning device.

Optimal operation occurs at rotor speed = 1500 rpm and gas velocity = 6 m/s, achieving 95–96 % efficiency.

The correlation between Re and Fr numbers provides a predictive model for design ptimization.

The developed design can be effectively used in cement, metallurgy, and chemical industries to ensure environmental compliance.

References

- 1. Sadullaev, X., Muydinov, A., Xoshimov, A., & Mamarizaev, I. (2021). Ecological environment and its improvements in the Fergana valley. Барқарорлик ва етакчи тадқиқотлар онлайн илмий журнали, 1(5), 100-106.
- 2. Askarov, X. A., Karimov, I. T., & Mo'Ydinov, A. (2022). Rektifikatsion jarayonlarining kolonnalarda moddiy va issiqlik balanslarini tadqiq qilish. Oriental renaissance: Innovative, educational, natural and social sciences, 2(5-2), 246-250.
- **3.** Tojiev, R., Alizafarov, B., & Muydinov, A. (2022). Theoretical analysis of increasing

- conveyor tape endurance. Innovative Technologica: Methodical Research Journal, 3(06), 167-171.
- **4.** Ахунбаев, А., & Муйдинов, А. (2022). Определение мощности ротора в роторнобарабанном аппарате. Yosh Tadqiqotchi Jurnali, 1(5), 381-390.
- **5.** Муйдинов, А. (2022). Экспериментальное исследование затрат энергии на перемешивание. Yosh Tadqiqotchi Jurnali, 1(5), 375-380.
- 6. Ахунбаев, А., & Муйдинов, А. (2022). Уравнения движения дисперсного материала в роторно-барабанном аппарате. Yosh Tadqiqotchi Jurnali, 1(5), 368-374.
- 7. Ахунбаев, А. А., & Муйдинов, А. А. У. (2022). Затраты мощности на поддержание слоя материала в контактной сушилке. Universum: технические науки, (6-1 (99)), 49-53.
- 8. Ergashev, N. A., Xoshimov, A. O. O. G. L., & Muydinov, A. A. O. (2022). Kontakt elementi uyurmali oqim hosil qiluvchi rejimda ishlovchi hoʻl usulda chang ushlovchi apparat gidravlik qarshilikni tajribaviy aniqlash. Scientific progress, 3(6), 94-101.

- 9. Ergashev, N. A., Mamarizayev, I. M. O., & Muydinov, A. A. O. (2022). Kontakt elementli hoʻl usulda chang ushlovchi apparatni sanoatda qoʻllash va uning samaradorligini tajribaviy aniqlash. Scientific progress, 3(6), 78-86.
- **10.** Axmadjonovich, E. N., Obidjon oʻgʻli, X. A., & Abduqayum oʻgʻli, A. M. (2022). Industrial application of dust equipment in the industrial wet method with contact elements and experimental determination of its efficiency. American Journal of Applied Science and Technology, 2(06), 47-54.